18

Power and Spectral Efficient Multiuser Broadband Wireless Communication System

Santi P. Maity
Bengal Engineering & Science University, Shibpur
India

1. Introduction

Communication Satellite plays significant role in long distance broadband signal transmission in recent times. Development of an efficient high data rate communication system for multiusers becomes important and challenging. To meet ever-increasing demand for broadband wireless communications, a key issue that should be coped with is the scarcity of power and spectral bandwidth. In the conventional communication scenario, supporting ubiquitous users with high quality data communication services requires huge bandwidth. However, since the spectrum of nowadays is a very costly resource, further bandwidth expansion is impracticable. Thus, the use of efficient multiple access is critical. Moreover, for a given limited bandwidth and limited number of antennas, the only option that can increase data rate is to increase transmit power as suggested by Shannon channel capacity theorem. Therefore, development of power and bandwidth efficient coding, modulation, and multiple-access techniques is essential for the future wireless communication systems implemented through Satellite link.

Considering the above issues, this chapter discusses a new communication system for Satellite system that can achieve high power and spectral efficiency in broadband wireless communication. To achieve the goal, development of a new and complete communication system with high user capacity and variable data rate become essential. The system includes multicarrier code division multiple access (MC-CDMA) with peak-to-average power ratio (PAPR) reduction using channel coding, optimization in MC-CDMA, estimation of wireless channel condition and MC-DMA with multi-user detection (MUD). The chapter proposal focuses on different aspects for different part of a communication system, namely PAPR reduction in transmitter, channel estimation for design of adaptive and optimized system, multiuser detection at the receiver for increase in user capacity. The different issues are described under four broad subheadings. Prior to that a brief literature review on the above issues are also presented.

The organization of the chapter is as follows: Section 2 presents literature review, while proposed system model is described in Section 3. Design of power and spectral efficient system is described in Section 4. Performance evaluation of the system is presented in Section 5, while conclusions and scope of future works are highlighted in Section 6.

2. Literature Review

In this section, we present a brief literature review related to PAPR reduction, multiuser detection in CDMA, channel estimation and optimization in CDMA/MC-CDMA system. The objective of this review is to discuss the merits and the limitations of the existing works, scope of the present work and finally to compare the performance of this work with respect to the related existing works.

A growing number of techniques have been proposed in the recent literature to alleviate power efficiency problem in multicarrier system through the development of PAPR reduction methods. The approaches include simplest filtering and clipping (Ochiai & Ima; 2000), partial transmit sequence (PTS) (Lim et al; 2006), selective mapping (Yoo; 2006) to the sophisticated trellis shaping approach (Ochia; 2004). Ochiai et al (Ochia; 2004) propose a new trellis shaping design based on recursive minimization of the autocorrelation sidelobes for reducing PAPR of the bandlimited orthogonal frequency division multiplexing (OFDM) signals. The exponentially increasing complexity of the PTS scheme prevents its use for MC-CDMA. Kang et al. (Kang et al; 2005) propose an efficient PTS scheme through phase factor optimization to reduce the complexity. Natarajan et al (Natarajan; 2004) address signal compactness issues in MC-CDMA employing CI codes using the measure of crest factors.

Literature on multiuser detection in CDMA is quite rich. The optimum multiuser detector proposed in (Vedu; 1986) achieves significant performance improvement relative to single user receiver but the computational complexity increases exponentially with the number of users. This has motivated the use of low complexity linear (Lupas & Vedu; 1989) and decision driven suboptimal multiuser detection techniques. To overcome the disadvantage intrinsic to the total parallel interference cancelation (PIC), some modified versions like partial parallel interference canceling (Divsalar et al; 1989) and linear parallel interference cancelation technique (Kim & Lee; 2001) have been proposed. Parallel interference weighted canceler has been proposed in (Xiao & Liang; 1999) to mitigate the degrading effects of unreliable interference estimation. Two variants of PIC known as threshold PIC and block PIC have been proposed in (Thippavajjula & Natarajan; 2004) for synchronous CI/MCCDMA uplink. Block PIC is shown to provide performance gain relative to conventional PIC. Maity et al (Maity at al; 2008a) further improves bit error rate (BER) performance of diversity assisted block PIC using genetic algorithms.

A growing number of techniques have been proposed in the recent literature to estimate wireless channel parameters. Sgraja et al (Sgraja & Linder; 2003) propose an algorithm to estimate the whole channel matrix using Wiener filtering. Such an estimator requires a Wiener filter, a multiplication operation for each element of the channel matrix and matrix inversion, which increases the complexity of the receiver for large number of sub-carriers. In some systems, a known training sequence is sent by the transmitter and a training algorithm is performed by the receiver on the observed channel output and the known input to estimate the channel (Chow et al; 1991), (Ziegler & Cioffi; 1992) The deterministic least squares (DLS) channel identification algorithm in (Ziegler & Cioffi; 1992) is such a simple but widely used training approach. However, it is not suited for time varying system. In (Wang & Ray; 1999), authors propose an adaptive channel estimation algorithm using the cyclic prefix. This algorithm can adaptively track the channel variation without additional training sequences.

In (Choi et al; 2001), time-domain channel estimation followed by symbol detection based on zero forcing (ZF) and minimum mean square error (MMSE) criterion have been proposed. Pilot based channel estimation is also widely used in many algorithms. The most common pilot based channel estimation scheme is the least square (LS) method of channel estimation

(Coleri et al; 2002), (Schramm et al; 1998). Blind adaptive channel estimation, based on least mean square (LMS) for OFDM communication, is proposed in (Doukopoulos & Moustakides; 2004). Kalman filter is also used for channel estimation in (Gupta & Mehra; 2007). Finite affine projection (FAP) algorithm is used to estimate the channel response for OFDM system in (Gao et al; 2007). Gao et al (Gao et al; 2007) propose an efficient channel estimation for multiple input multiple output (MIMO) single-carrier block transmission with dual cyclic timeslot structure. An optimal channel estimation is then investigated in the minimal mean square error (MMSE) sense on the time slot basis.
This channel state information (CSI) is exploited to design optimized system and several such algorithms for CDMA and MC-CDMA systems are reported in literature. The optimized systems include adaptive algorithm to minimize the total transmitted power (Lok & Wong; 2000), signal-to-interference ratio (SIR) balanced optimum power control in CDMA (Wu; 1999), joint optimization of spreading codes and a utility based power control (Reynolds & Wang; 2003), joint rate and power control (Kim; 1999), joint transmitter-receiver optimization using multiuser detection and resource allocation for energy efficiency in wireless CDMA networks (Buzzi & Poor; 2008), using transmitter power control, receiver array processing and multiuser detection (Seo & Yang,2006) etc. The objective of the optimized methods, in general, is to minimize transmit power and maximize per user's data transmission rate.

3. Proposed System

MC-CDMA system was first proposed in (Yee; 1993) and is a combination of CDMA and OFDM with the spreading codes applied in frequency domain. We use carrier interferometry (CI) code as spreading code. Interferometry, a classical method in experimental physics, refers to the study of interference patterns resulting from the superpositioning of waves. CI codes of length N supports N users orthogonally and then, as system demand increases, codes can be selected to accommodate upto addition N-1 users pseudo-orthogonaly. Additionally, there is no restriction on the length N of the CI code (i.e. $N \in I$), making it more robust to the diverse requirements of wireless environments. Since the present MC-CDMA system employs CI code as spreading code, this multiple access scheme is called as CI/MC-CDMA system. In other words, the CI/MC-CDMA is an MC-CDMA scheme employing complex carrier interferometry spreading codes. Assuming that there are K users and N subcarriers in the MC-CDMA system, the CI code for the k-th user $(1 \leq k \leq K)$ is given by (Natarajan et al; 2001):

$[1, e^{j\Delta}\theta_k, ...e^{j(N-1)\Delta}\theta_k]$ where $\Delta\theta_k = 2\pi.k/N$.

In this chapter, we have discussed the operation and performance of a newly developed CI/MC-CDMA model which is a variation that is discussed in (Natarajan et al; 2001). The system proposed here is capable of supporting high capacity with reduction in PAPR as well as low BER values at the receiver. Therefore, we present a brief review of the model in (Natarajan et al; 2001) followed by our new model.

3.1 Transmitter Model

In CI/MC-CDMA transmitter (Natarajan et al; 2001), the incoming data $a_k[n]$ for the k-th user, is transmitted over N narrow-band sub-carriers each multiplied with an element of the k-th user spreading code. Binary phase shift keying (BPSK) modulation is assumed, i.e. $a_k[n] = \pm 1$, where $a_k[n]$ represents n-th bit of k-th user. The transmitted signal corresponding to n-th bit of the incoming data is given by

$$S(t) = \sum_{k=0}^{N-1} \sum_{i=0}^{N-1} a_k[n] exp^{j(2\pi.f_i t + i\Delta\theta_k)} p(t) \quad (1)$$

where $f_i = f_c + i.\Delta f$ is the i-th subcarrier, and p(t) is a rectangular pulse of duration T_b. As with the traditional MC-CDMA, the Δf's are selected such that the carrier frequencies are orthogonal to each other, typically $\Delta f = 1/T_b$, where T_b is the bit duration.
The transmitter model developed in (Natarajan et al; 2001) allows high data rate transmission for (2N-1) users employing 'N' number of sub-carriers. However, in many practical situations, users may have transmission of variable data rate. It is logical to consider variable data rate transmission in multimedia signals environment as diverse classes of traffic signals have different requirement of quality of services (QoS)(Maity et al; 2008b). We like to modify the above transmitter model by allocating all sub-carriers to the users of high data rate transmission and odd and even sub-carriers are shared alternately among the users of low data rate. In other words, we can split the sub-carriers in even and odd parts as well as the 'N' length PO-CI (pseudo-orthogonal) codes in N/2 odd and N/2 even parts. The mathematical form for the transmitted signal S_1(t) becomes

$$S_1(t) = [\sum_{k=0}^{N-1} \sum_{i=0}^{N-1} a_k[n] exp^{j(2\pi.f_i t + 2\pi.i.k/N)} + \sum_{k=N}^{3N/2-1} \sum_{\forall i=odd}^{N-1} a_k[n] exp^{j(2\pi.f_i t + 2\pi.i.k/N + i\Delta\phi_1)}$$
$$+ \sum_{k=3N/2}^{2N-1} \sum_{\forall i=odd}^{N-1} a_k[n] exp^{j(2\pi.f_i t + 2\pi.(i+1).k/N + i\Delta\phi_2)} + \sum_{k=2N}^{5N/2-1} \sum_{\forall i=even}^{N-1} a_k[n] exp^{j(2\pi.f_i t + 2\pi.i.k/N + i\Delta\phi_3)}$$
$$+ \sum_{k=5N/2}^{3N-1} \sum_{\forall i=even}^{N-1} a_k[n] exp^{j(2\pi.f_i t + 2\pi.(i+1).k/N + i\Delta\phi_4)}] p(t - n.T_b) \quad (2)$$

where $\Delta\phi_1 = +\pi/2$,$\Delta\phi_2 = -\pi/2$,$\Delta\phi_3 = -\pi/N - \pi$ and $\Delta\phi_4 = -\pi/N$ indicate respective phase shift angles with respect to orthogonal CI codes. The phase shift are set in order to make the same even or odd subcarriers used by the different users through the respective spreading codes in out-of-phase. This out-of-phase condition reduces cross-correlation values among the spreading code patterns that not only leads to the reduction in PAPR values but also lower BER values at the receiver. This fact is analyzed mathematically as well as is supported by simulation results.

3.2 Channel Model

We also introduce here the channel model. The particular channel model needs to be considered since we will analyze later BER performance of the proposed system and its relative improvement/ degradation due to reduction in PAPR. An uplink model has been considered where all the users' transmissions are assumed to be synchronized for simplification of analysis, although, this condition may seem difficult to be valid practically. It is also assumed that every user experiences an independent propagation environment that is modeled as a slowly varying multipath channel. Multipath propagation in time translates into frequency selectivity in the frequency domain (Proakis, 1995). Frequency selectivity refers to the selectivity over the entire bandwidth of transmission and not over each subcarrier transmission. This is because $\frac{1}{T_b} \ll (\Delta f_c) \ll BW$, where Δf_c is the coherence bandwidth and BW is the total bandwidth.

3.3 Receiver Design for the proposed system

In this subsection, we describe the multiuser receiver operation when all the users transmit data through all sub-carriers as developed $S(t)$ in Eq. (1). The received signal $r(t)$ for this $S(t)$ corresponds to

$$r(t) = \sum_{k=1}^{K} \sum_{i=0}^{N-1} \alpha_{ik} a_k[n] cos(2\pi.f_i t + i.\Delta\theta_k + \beta_{ik}).p(t) + \eta(t) \tag{3}$$

where α_{ik} is the Rayleigh fading gain and β_{ik} is uniformly distributed phase offset of the k-th user in the i-th carrier and the symbol $\eta(t)$ represents additive white Gaussian noise (AWGN). The received signal is projected onto N-orthogonal carriers and is despread using j-th users CI code resulting in $r^j = (r_0^j, r_1^j, ...r_{N-1}^j)$, where r_i^j corresponds to

$$r_i^j = \alpha_{ij}.a_j[n] + \sum_{k=1,k\neq j}^{K} \alpha_{ik} a_k[n] cos(i(\Delta\theta_k - \Delta\theta_j) + \beta_{ik} - \hat{\beta}_{ij}) + \eta_i \tag{4}$$

where η_i is a Gaussian random variable with mean 0 and variance $N_0/2$. Exact phase and frequency synchronization for the desired user is assumed i.e.,$\hat{\beta}_{ij} = \beta_{ij}$. Now, a suitable combining strategy is used to create a decision variable D_j, which then enters a decision device that outputs $\hat{a}_j$. Minimum mean square error combining (MMSEC) is employed as it is shown to provide the best performance in a frequency selective fading channel (Cal & Akansu; 2000). The decision variable D_j for the n-th bit is (Natarajan et al; 2001)

$$D_n^j = \sum_{i=1}^{N} r_i^j w_{ij} \tag{5}$$

where

$$w_{ij} = \frac{\alpha}{(var(a_k)A_{ij} + N_0/2)} \tag{6}$$

where $A_{ij} = \sum_{k=1}^{K} \alpha_{ik}^2 cos(i\delta\theta_k - i\delta\theta_j + \beta_{ik} - \beta_{ij})^2$ and $var(a_k) = 1$. Thus, the outputs as the single user detector for all the users generate a decision vector $D = [D^1, D^2, ...D^K]$ which is used to obtain the initial estimates of the data $\hat{a} = (\hat{a}_1, \hat{a}_2, ...\hat{a}_k)$. These initial estimates are then used to evaluate multiple access interference (MAI) experienced by each user in the interference cancelation technique.

4. Design of power and spectral efficient system

This section describes multi-carrier code division multiple access (MC-CDMA) with PAPR (peak-to-average power ratio) reduction using channel coding, optimized system design for number of subcarriers and users, estimation of wireless channel condition, and finally MC-CDMA with multi-user detection (MUD). The overall discussion focuses on different issues for different section of a communication system, namely PAPR reduction and optimized system design in transmitter, estimation of parameters for the channel, multiuser detection at the receiver for increase in user capacity. The different issues are described under four broad subheadings as follows.

4.1 MC-CDMA with PAPR reduction using channel coding

In this section, we will first define PAPR mathematically and then see whether this PAPR is related to the properties of the spreading codes in multiuser systems. The rationale behind such relation lies as each subcarrier is multiplied by chip of individual user's spreading code which is generated from phase shift for CI codes. It would not be irrelevant to mention here that high PAPR occurs due to the superpositioning of several in-phase or near in-phase subcarriers. So cross-correlation and auto-correlation values of CI codes expect to have an influence on PAPR values of the resultant multiuser signals. In MC-CDMA system, the corresponding PAPR definition per discrete-time symbol is given by

$$PAPR = \frac{\max_{0\leq i\leq N-1}|S(i)^2|}{E[S(i)^2]} \tag{7}$$

where $E[|S(i)|^2]$ and $\max_{0\leq i\leq N-1}|S(t)|^2$ denote the the average power and the peak power, respectively in one symbol interval. The power of i-th time-domain sample denoted by $P(i)$, $1 \leq n \leq N$, from equation (2) for complex signal is

$$\begin{aligned} P(i) &= (\sum_{k=1}^{K}\sum_{i=0}^{N-1} a_k[n]c_k^i exp(j2\pi f_i t))(\sum_{k=1}^{K}\sum_{i1=0}^{N-1} a_k[n]c_k^i exp(j2\pi f_i t))^* \\ &= \sum_{k=1}^{K}|a_k[n]|^2 + \sum_{k=1}^{K}\sum_{k=1,k\neq k1} a_k[n]a_{k1}[n] \sum_{i2=-(N-1)}^{N-1} Z^{(k,k1)}(i2)exp(i2\pi f_{i2}t) \\ &\quad + \sum_{k=1}^{K} a_k[n]^2 \sum_{i2=-(N-1),i2\neq 0}^{N-1} Z^{(k,k)}(i2)exp(j2\pi f_{i2}t) \end{aligned} \tag{8}$$

The symbol $a_k[n]$ indicates n-th symbol of k-th user. Here $Z^{k,k1}(i2)$ is the aperiodic crosscorrelation function of spreading codes between user k and k1,

$$Z^{(k,k1)}(i2) = \sum_{m=1}^{N-i2} c_k^m (c_{k1}^{m+i2})*$$

and $Z^{k,k}(i2)$ is the aperiodic autocorrelation function of the k-th user. It can be found that the signal power of MC-CDMA system is partially determined by the correlation property of the selected set of spreading codes. We now briefly present proposed PAPR reduction method using code optimization, phase optimization and trellis coding.

A. Code Optimization

As defined earlier, the CI code for the k^{th} user is given by the spreading sequence,

$$\begin{aligned} \{\beta_k^0, \beta_k^1, \beta_k^2, ...\beta_k^{N-1}\} &= \{e^{j\Delta\theta_k^0}, e^{j\Delta\theta_k^1}...e^{j\Delta\theta_k^{N-1}}\} \\ &= \{e^{j(2\pi/N)0.k}, e^{j(2\pi/N)1.k}...e^{j(2\pi/N)(N-1).k}\} \end{aligned} \tag{9}$$

Here, $k\epsilon[0, 1, 2, ...K-1]$. However, low value of PAPR is achieved if we give cycle shift of the code that leads to new code. We can write the new code as

$$\begin{aligned} \text{New code } &= \{\beta_{k+shift}^0, \beta_{k+shift}^1, ...\beta_{k+shift}^{N-1}\} \\ &= \{e^{j\Delta\theta_{k+shift}^0}, e^{j\Delta\theta_{k+shift}^1}...e^{j\Delta\theta_{k+shift}^{N-1}}\} \\ &= \{e^{j(2\pi/N)0.(k+shift)}, e^{j(2\pi/N)1.(k+shift)}... \\ &\qquad e^{j(2\pi/N)(N-1).(k+shift)}\} \end{aligned} \tag{10}$$

Here 'shift' indicates the number of cycle shift which is fixed for all users for a given period of time, $[0 \leq' shift' \leq K]$. It is seen from the simulation results that for a minimum value of PAPR, the 'shift' is either [1,2,3] or [(K-1) to (K-3)]. It is also found that performance achieved by doing (K-1) to (K-3) shifting operations is same as is obtained by performing 1 to 3 times reverse shifting. This means that as far as the code optimization is concerned, code sequence for the users is shifted in forward or reverse cyclic shifting by an amount of 1 to 3 shifts.

B. Phase Optimization

To achieve lower PAPR value, we can use the iterative method where we shift the phase of each set of users with additional rotation in between $\Delta\phi_{(max)}$ and $\Delta\phi_{(min)}$ so that the condition $\Delta\phi_{(max)} > \Delta\phi > \Delta\phi_{(min)}$ is satisfied. It is also to be mentioned here that $\Delta\phi_{(max)}$ is allowed to take value of $\Delta\phi + \pi/32N$, while $\Delta\phi_{(min)}$=$\Delta\phi - \pi/32N$. Fig. 1 shows the proposed code and phase optimized variable data rate CI/MC-CDMA system with reduction in PAPR value.

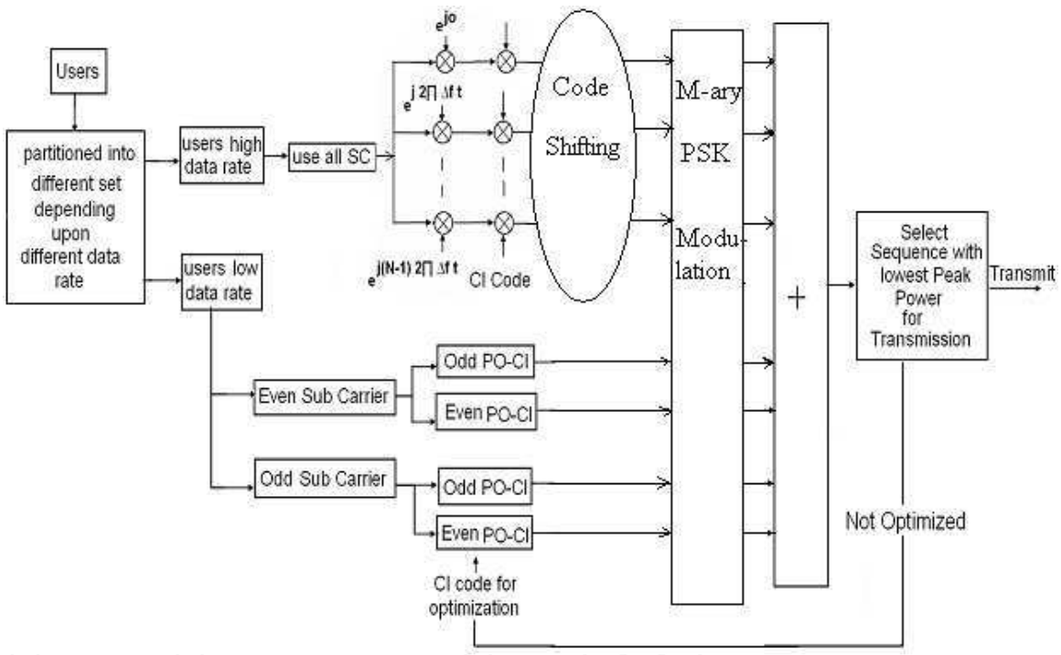

Fig. 1. Block diagram representation of proposed M-ary CI/MC-CDMA PAPR reduction scheme

C. Trellis coding

We also incorporate the effect of trellis coding for further improvement in PAPR reduction. Trellis coding is a kind of convolution coding used here in combination with code and phase optimization so that symbols for the different users are placed in the constellation that may minimize the occurrence of high peak generation in the same odd and even sub-carriers. Moreover, the usage of trellis coding offers the benefit of reduction in bit error rate (BER) performance at the receiver. Fig. 2 shows the simplified block diagram of Fig. 1 with trellis coding.

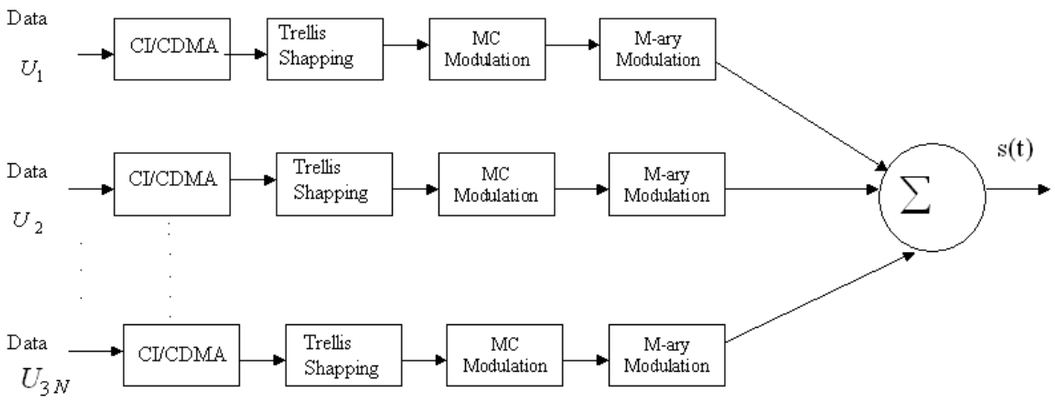

Fig. 2. Simplified block diagram representation for the proposed M-ary CI/MC-CDMA scheme with trellis coding

4.2 Proposed GA based channel estimation

This subsection first defines fitness function 'F' and GA based minimization is presented later.

A. Formation of Fitness function

We assume that actual fading gain at n-th subcarrier is α_n and its estimated value is denoted by $\hat{\alpha}_n$. The error in estimated value is represented by e_n. We can think of probability density function (pdf) of the estimation error as central Chi-square distribution (Ahamad & Assaad; 2009) and can be written as follows:

$$f(|e_n^2|) = \frac{1}{\sigma_n^2} e^{\frac{-|e_n|^2}{\sigma_n^2}} \tag{11}$$

where σ_n^2 is the variance of estimation error. So, in terms of estimated channel gains and its corresponding error terms, the expression of (4) can be written as follows:

$$\begin{aligned} r_i^j &= \hat{\alpha}_i + e_i + \sum_{k=1,k\neq j}^{K} \hat{\alpha}_i \rho_{kj} + \sum_{k=1,k\neq j}^{K} e_i \rho_{kj} + \eta_j \\ &= \hat{\alpha}_i + e_n + \sigma_I^2 + \sigma_{Ie}^2 + \sigma_N^2 \end{aligned} \tag{12}$$

The first, second, third, forth and fifth term of (12) can be designated for the j-user as signal term in $i-$ th subcarrier, estimated error in signal term, variance of interfere i.e. interference power due to all other users at i-th subcarrier, interference power for estimation error, and noise power at i-th subcarrier, respectively. For large number of users, the third and the forth term correspond to a random variable with normal distribution (according to central limit theorem).

We define signal-to-interference noise power ratio (SINR) corresponding to j-th user's bit at i-th subcarrier as follows:

$$(SINR)_i^j = \frac{(|\hat{\alpha}_i| + |e_i|)^2}{\sigma_I^2 + \sigma_{Ie}^2 + \sigma_{N_i}^2} \tag{13}$$

We assume SINR for all subcarriers are independent, so total SINR for j-th user's bit is

$$(SINR)^j = \sum_{i=1}^{N} (SINR)_i^j \tag{14}$$

The channel capacity corresponding to j-th user's is

$$C^j = log(1 + SINR^j)\ bits/sample \tag{15}$$

Now total channel capacity can be calculated as $C = \sum_{\forall j} C^j$.
We now define 'F' as weighted average of channel capacity and detection probability p_e i.e. $F = f(C, p_e)$. It is preferable to minimize 'F', while target is to maximize C and minimize p_e. It is logical to express C as $C_{norm} = \frac{C_{\hat{\alpha},e}}{C_{\alpha=1}}$, that indicates normalization of the channel capacity. The symbol $C_{\alpha=1}$ corresponds to non-fading situation and obviously channel capacity with reliable decoding will be high. It is quite true that the value of $\frac{C_{\hat{\alpha},e}}{C_{\alpha=1}}$ is less than 1 but our target is to achieve this value close to 1. The p_e is calculated as follows:

$$p_e = \frac{1}{K}\sum_{k=1}^{K}(b_k - \hat{b}_k) \tag{16}$$

where, K is total number of users, b_k and $\hat{b}_k$ are the transmitted and the received k-th user bit, respectively.
The objective function 'F' can be defined as

$$F = w_1(1 - C_{norm}) + w_2 p_e = w_1(1 - \frac{C_{\hat{h},e}}{C_{h=1}}) + w_2 p_e \tag{17}$$

where w_1 and w_2 are the weight factors of channel capacity and detection reliability, respectively. Each weight factor represents how important each index is during the searching process of GA. For example, if both indices are equally important, each one should be 0.5 so that the relationship $w_1 + w_2 = 1.0$ must hold.
B. Optimization of Fitness function using GA
The experimental conditions of GA for the present problem are depicted as follows:
(i) size of population is 10,(ii) number of generation/iterations 100, (iii) probability of crossover per generation is 0.80, and (iv) probability of mutation per bit is 0.07.
Initialization of twenty sets of random values for $\hat{\alpha}_1$,$\hat{\alpha}_2$,.....$\hat{\alpha}_n$, e_1,e_2,.....e_n are done. The values of $\hat{\alpha}_i$ are taken from Rayleigh distribution, while the values of e's are taken from (11). Then the value of C and p_e are calculated for each set. Using the procedure outlined in previous subsection, the value of fitness function 'F' is calculated for each of $\hat{\alpha}_1$,$\hat{\alpha}_2$,.....$\hat{\alpha}_n$, e_1,e_2,.....e_n using (17). An upper bound of F value (F_U) is determined based on the calculated 'F' values. The value of (F_U) acts as a threshold and is adjustable. This is required so that the needful number of sets of $\hat{\alpha}_1$,$\hat{\alpha}_2$,.....$\hat{\alpha}_n$, e_1,e_2,.....e_n values for which 'F' values lie below the (F_U) are duplicated. The remaining sets having 'F' values higher than (F_U) are ignored from the population. This process is done from the concept of selection of GA based algorithm. A binary string is generated through decimal-to-binary conversion for each selected set of $\hat{\alpha}_1$,$\hat{\alpha}_2$,.....$\hat{\alpha}_n$, e_1,e_2,.....e_n value and thus a set of strings are calculated for all selected combinations. Now, crossover and mutation operations are done with above probabilities.Operations as described, when applied to the selected sets, generate a new set of $\hat{\alpha}_1$,$\hat{\alpha}_2$,.....$\hat{\alpha}_n$, e_1,e_2,.....e_n value. This set is considered as population for next iteration/generation of the proposed GA based optimization problem. The operations are repeated for desired number of iterations or till a predefined acceptable values for C and p_e are achieved.

4.3 Subcarrier PIC scheme

Multicarrier (MC) signal can be modeled as a vector in N-dimensions where N-mutually orthogonal subcarriers form the basis signals. Accordingly, MC-CDMA signals with high and low data rates can be modeled as vectors of different dimensions in subcarrier signal space. In MUD, CDMA signal is treated as a vector and is projected onto individual orthogonal spreading function to estimate the interference of other users for the respective user. In PIC, for a given user, CDMA composite signal is projected simultaneously to all spreading codes except the desired one and the process demands high computation cost. The multiple access interference (MAI) estimation and its subsequent cancelation in MC-CDMA with variable data rates can be implemented in the respective subcarrier component rather than projecting it onto spreading functions followed by calculation of vector magnitude (Eq. 5 and Eq. 6), as is done in case of conventional PIC method. This very simple concept is used to develop a low computation cost PIC scheme when MAI is subtracted at the sub-carriers level. Fig. 3 shows the block diagram representation of the proposed PIC method. The users are divided in two different blocks, block 1(B-1) with high data rate transmission and block-2 (B-2) with low data rate transmission.

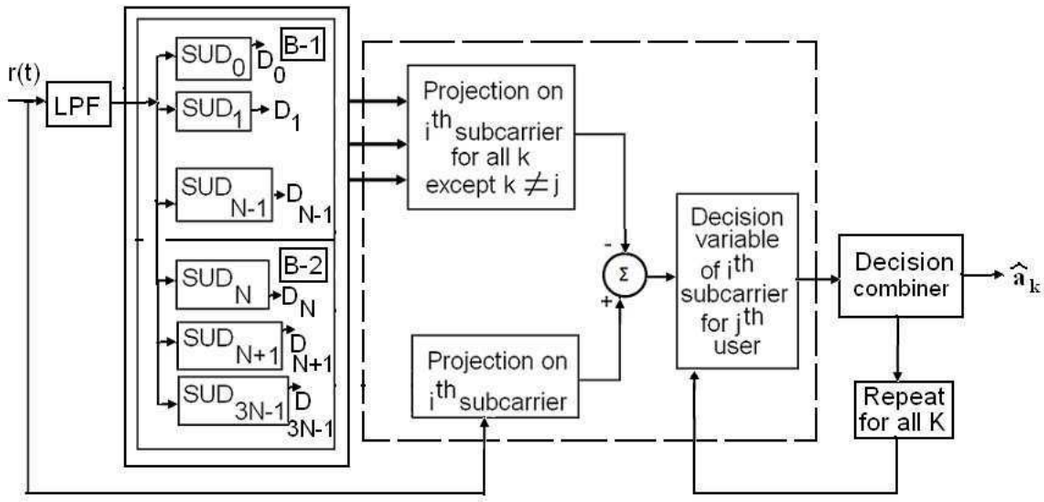

Fig. 3. Block diagram representation of proposed PIC scheme

The received multiuser signal $r(t)$ is first passed through a lowpass filter followed by single user detection through MMSEC. The decision vector $D = [D^1, D^2, ...D^K]$ then generates the initial estimates of the data $\hat{a} = (\hat{a}_1, \hat{a}_2, ...\hat{a}_k)$ which are used to determine the polarity of the interference. To estimate the interference experienced by j-th user at i-th subcarrier, the received signal r(t) and the signal of all other users, except the j-th user, are projected onto i-th subcarrier. The interference of other users are subtracted collectively from the former.
We now analyze mathematically the interference free estimation for the n-th bit of j-th user for conventional PIC, two block PIC and the proposed subcarrier PIC. The expression of the same for the conventional PIC system is

$$\hat{a}_n^j = r_n - \sum_{k=1,k\neq j}^{K} \hat{a}_n^k \tag{18}$$

The similar expression for an arbitrary j-th user belonging to strong group and when belong to weak group, respectively (of a two block PIC system) can be written as follows:

$$\hat{a}_n^j = r_n - \sum_{\forall k_1 \in S_1, k_1 \neq j} \hat{a}_n^{k_1} \tag{19}$$

$$\hat{a}_n^j = r_n - \sum_{\forall k_1 \in S_1} \hat{a}_n^{k_1} - \sum_{\forall k_2 \in S_2, k_2 \neq j} \hat{a}_n^{k_2} \tag{20}$$

where the symbols of $\hat{a}_n^j, r_n$, S_1 and S_2 represent n-th estimated bit of j-th user, resultant received signal for n-th bit, set of strong and weak user groups, respectively.
The interference free estimation of the i-th subcarrier for the j-th user of block B_1,

$$r_i^j = r_i - \sum_{\forall k_1 \in B_1, k_1 \neq j} r_i^{k_1} \tag{21}$$

while the expression for the same belonging to block B_2,

$$r_i^j = r_i - \sum_{\forall k_1 \in B_1} r_i^{k_1} - \sum_{\forall k_2 \in S_2, k_2 \neq j} r_i^{k_2} \tag{22}$$

where r_i^j and r_i indicate the i-th subcarrier component of the j-th user and the i-th subcarrier component of resultant received signal, respectively.

Now, the decision variable D_n^j for the n-th bit of an arbitrary j-th user of block B_1 can be written accordingly to Eq. (5). The equation is rewritten in Eq. (22) for convenience of further analysis. The similar expression for the j-th user of the block B_2 is written in Eq.(23)

$$D_n^j = \sum_{i=1}^{N} r_i^j w_{ij} \tag{23}$$

$$D_n^j = \sum_{\forall i = odd\ or\ even}^{N} r_i^j w_{ij} \tag{24}$$

The values of r_i^j in Eq. (22) and Eq. (23) can be put from Eq. (20) and Eq. (21), respectively.

Mathematical analysis of Eq. (20)-Eq.(23) show that stable decision variable D_n^j can be achieved for subcarrier PIC method compared to conventional PIC and block PIC. This is because interference due to other users are subtracted before forming D_n^j in the case of former unlike the latter methods where D_n^j is formed first and then interference is subtracted. This stable decision variable D_n^j gives rise to better estimation of $\hat{a}_j$ leading to an improvement in BER through interference cancelation. Moreover, the computation cost and time requirement is less compared to the conventional PIC and other block PIC (Thippavajjula; 2004). This can be well understood considering the fact that the users of block-1, transmit data at 'q' times higher rate (say) compared to the users of block-2. So, for 'q' consecutive bits detection of high data rate users, estimated interferences for the single bit due to low data rate users can be made use. In other words, interferences estimated for low users' single bit can be applied to improve subsequent BER of high user data. It is to be mentioned here that the projection of the received signal on the mutually orthogonal subcarriers is essentially the same for both

the conventional PIC and the proposed PIC. However, the interference in the former is subtracted after combining them as decision vector while in the later, interference is subtracted in subcarrier level itself. The computation complexity, for CI codes of length N, is $O(2N-1)$ for conventional PIC, 2 $O(N)$ for block PIC (Thippavajjula; 2004) and $O(N)$ for the proposed subcarrier PIC.

4.4 Optimized system design

In the present study, optimum values for N, K, and SNR are calculated based on the minimization of a fitness function 'F' that depends on PAPR, BER and average data rate (ADR). We first define 'F' and then GA based minimization technique is presented. Let us define the following symbols:
P_{diff}: Difference in threshold PAPR and actual PAPR
B_{diff}:Difference in threshold BER and actual BER
ADR:Average data rate which is normalized with respect to the collective data of all users transmitting at high data rates.
The predefined values of PAPR and BER indicate threshold of the permissible values for the respective parameters. It is to be noted that we have considered P_{diff} and B_{diff}, instead of considering their actual values, while forming the objective function and its subsequent minimization process is performed. This is done so as these two measures are related in a conflicting manner with their associated parameters and the simultaneous minimization of both of these is not optimally achievable with respect to the overall optimal system design is concerned. So the objective is to reduce P_{diff} and B_{diff} whether their actual values are below or above the threshold value. The fitness function 'F' is defined as follows:

$$F = w_1 P_{diff} + w_2 B_{diff} + w_3(1 - ADR) \tag{25}$$

where w_1,w_2 and w_3 are defined as follows:

$$w_1 = \frac{B_{diff} \times (1 - ADR)}{(P_{diff} + B_{diff})(1 - ADR) + B_{diff} P_{diff}} \tag{26}$$

$$w_2 = \frac{P_{diff} \times (1 - ADR)}{(P_{diff} + B_{diff})(1 - ADR) + B_{diff} P_{diff}} \tag{27}$$

$$w_3 = \frac{P_{diff} \times B_{diff}}{(P_{diff} + B_{diff})(1 - ADR) + B_{diff} P_{diff}} \tag{28}$$

so that $0 < w_1$,w_2,$w_3 < 1$ and w_1+w_2+$w_3 = 1$ relation must hold.
The values of w_1,w_2 and w_3 when put in Eq. (24), the expression of 'F' becomes

$$F = \frac{3P_{diff} \times B_{diff} \times (1 - ADR)}{(P_{diff} + B_{diff})(1 - ADR) + B_{diff} P_{diff}} \tag{29}$$

We now describe very briefly GA based optimization process. Initialization of twenty sets of random $\{N, K, SNR\}$ values within the predefined range are done. The values for P_{diff}, B_{diff} and ADR as well as the value of fitness function 'F' for each set of {N,K,SNR} are then calculated. A predefined threshold (F_U) value of 'F' is assigned to identify the fit parameter sets. The particular sets of {N,K,SNR} for which 'F' values lie below the F_U are duplicated and the other sets are ignored from the population following the spirit of GA. Now, crossover

and mutation operations are done on the strings. The experimental conditions of GA for the present problem are depicted as, (i) size of population is 20, (ii) probability of crossover per generation is 0.80, and probability of mutation per bit is 0.09, user capacity i.e. number of users vary from 15-75, number of subcarriers range from 10-25, value of SNR range from 7-14 dB. The operations are done for the desired number of iterations or till a predefined acceptable values for PAPR and BER are achieved for optimal values of N, K and SNR.

5. Performance Evaluation

In this section, we present performance analysis of PAPR reduction, channel estimation, subcarrier PIC for improved receiver operation and finally optimization system for power and spectral efficient system design.

5.1 Performance for PAPR reduction

This subsection presents the performance of the proposed PAPR reduction technique in synchronous M-ary CI/MC-CDMA system. As figures of merit, we evaluate the complementary cumulative distribution function (CCDF) of PAPR under various phase modulation. We also show through simulation results that the proposed CI/MC-CDMA method offers lower PAPR and BER values compared to conventional CI/MC-CDMA system (Natarajan et al; 2001) and other recent work [12]. We first show the cross-correlation values for the different user's spreading codes under the phases as described in equation (7). The cross correlation (CC) between user k's signature waveform $c_k(t)$[created using the spreading sequence (1, $e^{j\Delta}\theta_k$,... $e^{j(N-1)\Delta}\theta_k$) and user j's signature waveform [created via the spreading sequence (1, $e^{j\Delta}\theta_j$,... $e^{j(N-1)\Delta}\theta_j$) can be shown as follows

$$R_{k,j}(\tau) = \frac{1}{2\Delta f} \sum_{i=0}^{i=N-1} cos(i(2\pi.\Delta f\tau)) \tag{30}$$

$$R_{k,j}(\tau) = \frac{1}{2\Delta f} \frac{sin(1/2N.2\pi.\Delta f.\tau)}{sin(1/2.2\pi.\Delta f.\tau)} cos(\frac{(N-1)}{2} 2\pi\Delta f\tau) \tag{31}$$

where $\tau = \Delta t_k - \Delta t_j = (\Delta\theta_k - \Delta\theta_j)/2\pi.\Delta f$. Table 1 shows the cross-correlation values for some arbitrary pair of spreading codes under various phase shifts. Numerical values show that $R_{j,k}$ values are reduced significantly for the proposed phase shifts of the code patterns.

We now show cumulative complementary distribution function (CCDF) of PAPR values for different M-ary modulations with separate code and phase optimization of the spreading codes in Fig. 4 and as well as with the combined effect of code and phase optimization in Fig. 5. It is also to be mentioned here that the proposed PAPR reduction algorithm is very fast. It takes approximately 2.25 second for 10 time iteration in MATLAB 7 platform running on a Pentium IV 2.79 GHz, 512 MB RAM PC system. The graphical representation shows that best PAPR reduction performance is achieved for the proposed algorithm with QPSK system, while the worst PAPR reduction performance is shown in BPSK performance. Similarly, PAPR reduction performance of 16-ary PSK is comparatively better than 8-ary PSK system. The results obtained are quite consistent with the cross-correlation values shown in the Table 1 for any arbitrary pair of code patterns and different M-ary modulation. While phase quadrature in QPSK system is not much influenced by the polarity of the symbols, but in case of BPSK modulation the polarity of symbols makes superimposition of subcarriers for in-phase that leads to an increase in PAPR value. It is interesting to see that for BPSK, QPSK and 8-ary PSK

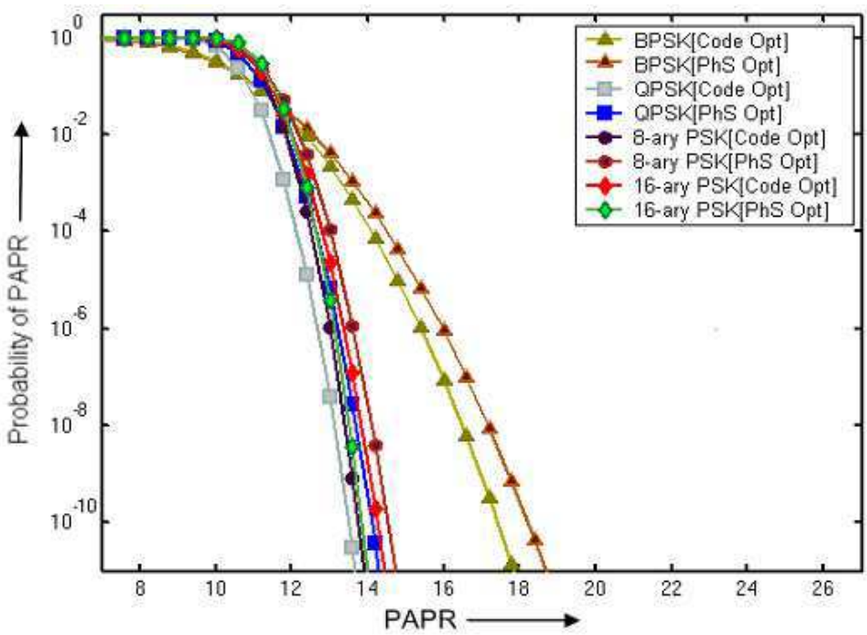

Fig. 4. CCDF of PAPR for N=8 and K=24 with code and phase optimization separately

code optimizations are more effective for reduction in PAPR values. On the other hand, for 16-ary PSK, phase optimization is more effective. Significant improvement in PAPR reduction is possible to achieve by exploiting the combined effect of code and phase optimization. Fig. 5 shows that PAPR values are not only reduced but also the probability for the PAPR values over a particular threshold value also become low. Fig. 6 shows improvement in PAPR using trellis coding.

We also test PAPR reduction performance of the proposed system in real time system of Agilent made N5182A MXG RF vector signal generator (VSG). The signal characteristics is 100 kHz to 3 GHz, +23 dBm output power at 1GHz = -121 dBc/Hz (typ), phase noise at 1 GHz and 20 kHz offset =1.2 ms switching speed in SCPI mode; $\leq$ 900 micro-second simultaneous frequency, amplitude, and waveform switching in list mode. Fig. 7 shows CCDF for PAPR reduction when the proposed algorithm is generated in VSG before code and phase optimization while the same is shown in Fig. 8 after code and phase optimization. The results show that due to optimization peak power is not only reduced from 6.37 dB to 4.06 dB, but also probability for attaining 0dB value also increases from 37% to 46 %. Similarly, 10% probability is found for PAPR value with 3.52dB, while after optimization this value reduces to 3.06dB. So theoretical performance improvement of PAPR reduction is also verified in hardware system indicating the importance of implementation of the proposed algorithm in practical system.

PAPR reduction for the proposed algorithm is also verified in VSG for 8-ary PSK modulation. Results are shown in Fig. 9 and Fig. 10. The results show that due to optimization not only peak power is reduced from 7.27 dB to 6.13 dB, but also probability for attaining 0dB value increases from 29% to 35 %. Similarly, 10% probability is found for PAPR value with 3.35dB, while after optimization this value reduces to 3.00dB. Verification results once again support the theoretical results that PAPR reduction performance for the proposed algorithm with 8-ary and 16-ary modulation system lie between performance for BPSK and QPSK modulation.

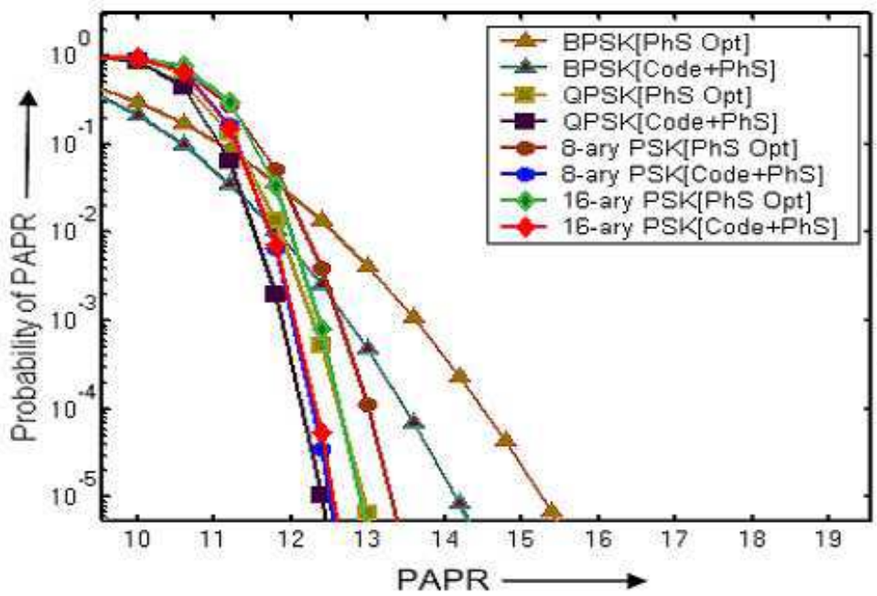

Fig. 5. CCDF of PAPR for N=8 and K=24 with combined code and phase optimization

5.2 Performance evaluation for channel estimation

This subsection represents performance analysis of the proposed channel estimation method. We have evaluated BER for different number of users at SNR=7dB and the number of subcarriers N=10. Fig. 11 shows that BER values corresponding to the estimated channel parameters become more closer to the values corresponding to the actual values of the channel parameters. Simulation results show that for N=10, difference in BER value corresponding to the actual and the estimated channel parameters become of the order of 0.085 for the number of users 20, and is of the order of 0.055 for the number of users 30. We also test the effect of the number of iterations/generations on the estimated channel parameters in terms of detection reliability and channel capacity. Fig. 12 shows that BER values increase with the increase of number of users but decreases with the number of generations. At the same time normalized (maximum values is 1) data transmission capacity is increased significantly with the number of generations which is shown in Fig. 13.

We also compare performance of the proposed method with the method in (Doukopoulos & Moustakides; 2004). For compatibility, orthogonal frequency division multiplexing (OFDM) system of (Doukopoulos & Moustakides; 2004) is designed as MC-CDMA system for the same number of subcarriers N=10 and simulation is performed at SNR=7 dB. Simulation results shown in Fig. 14 reflects the fact that the proposed channel estimation offers better BER performance due to the optimal selection of GA. The computation complexity for the proposed method is $O(n)$, while the same for LMS method in (Doukopoulos & Moustakides; 2004) is $O(n^2)$.

5.3 Performance evaluation of subcarrier PIC

Fig. 15 shows BER performance of the proposed scheme at 14 dB SNR and with N=16 subcarriers for 3N users system where N number of users transmit high data rate and 2N number of users transmit low data rate. The graphical result shows that when capacity is low (less

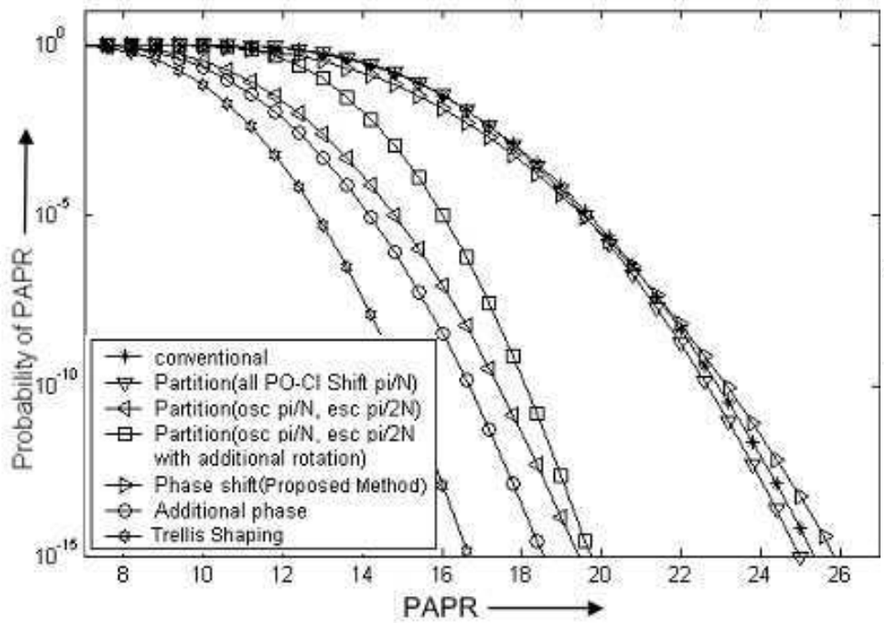

Fig. 6. CCDF of PAPR for N=8 and K=24 using trellis coding

than 20 users), MMSEC receiver of conventional CI/MC-CDMA system (shown as Con. MMSEC in the figure) performs significantly better compared to MMSEC receiver of the proposed system (shown as MMSEC in the figure). This is due to the fact that all users in the former transmit data using all sub-carriers while some of the users in the latter transmits data using either odd or even sub-carriers. However, significant improvement in BER performance is achieved in the latter case compared to the former when the number of users are gradually increasing over 20. Further significant improvement in BER performance can be achieved after different stages of the proposed subcarrier PIC scheme. Simulation results show that the proposed subcarrier PIC scheme after third stage iteration, can support the number of users three times the number of sub-carriers with BER of the order of 0.0428 (0.11071 for (Natarajan et al; 2001)), and it can support users upto four times the number of sub-carriers with BER of the order of 0.1350 (0.2193 for (Natarajan et al; 2001)).

We also test BER performance of the proposed scheme with the increase of number of users transmitting at high data rate. Fig. 16 shows BER performance of the proposed scheme at SNR 14 dB with N=16 sub-carriers for 2.5N users system. Here 1.5 N number of users transmit at high data rate and N number of users transmit low data rate. Simulation results show that the system supports the number of users two-and-half and three times the number of sub-carriers with BER values of 0.0591 and 0.104, respectively after three stage iterations. The relative degradation in BER performance for 2.5 N system, over 3N system, based on the proposed subcarrier PIC is due to the increase in overall data transmission rate for the former compared to the latter. The over all data transmission rate is 0.7742 times for 3N user and 0.9032 times for 2.5 N system with respect to the conventional CI/MC-CDMA system (Natarajan et al; 2001). The numerical values specified here for data transmission rate is obtained when transmission rate between high and low data rate user differs by a factor of 4.

We also compare BER performance of the proposed subcarrier PIC scheme (SCPIC) and block PIC (BPIC) scheme (Thippavajjula; 2004). The results are reported with the performance of

Arbitrary code pairs	Diff. PSK Sys.	Two Ort. cod. (j,k)	Orth.Code (j) $\pm\pi/M$ Shift. codes	$+\pi/M$ & $-\pi/M$.shift. codes
1st pair	BPSK	0.3953	0.3750	0.3536
	QPSK	0.2812	0.2789	0.2542
	8- PSK	0.3162	0.3149	0.3020
	16- PSK	0.3617	0.3411	0.3211
2nd pair	BPSK	0.3953	0.3750	0.3536
	QPSK	0.2834	0.2791	0.2590
	8- PSK	0.3179	0.3151	0.3001
	16- PSK	0.3619	0.3459	0.3291
3rd pair	BPSK	0.3953	0.3750	0.3536
	QPSK	0.2834	0.2791	0.2590
	8- PSK	0.3179	0.3151	0.3001
	16- PSK	0.3619	0.3459	0.3291
4rth pair	BPSK	0.3962	0.3690	0.3542
	QPSK	0.2842	0.2709	0.2581
	8- PSK	0.3287	0.3124	0.3054
	16- PSK	0.3754	0.3589	0.3205

Table 1. Cross correlation values for arbitrary code pair

Sl. no	N	K	SNR	PAPR	BER	ADR
1	22	64	10	10.2649	0.0482	0.7444
2	24	70	10	11.4017	0.0450	0.6700
3	21	60	14	10.0973	0.0125	0.8100
4	23	68	14	11.4012	0.0650	0.5000
5	18	52	11	10.4698	0.0464	0.5577
6	21	65	12	10.8132	0.0414	0.5407
7	23	67	12	11.7433	0.0701	0.5135
8	19	57	14	10.066	0.0422	0.5716

Table 2. GA based optimization for the proposed method

(Natarajan et al; 2001) through interference cancelation (IC). Fig. 17 shows that BER performance of the proposed subcarrier PIC scheme is significantly better compared to that of block PIC scheme and needless to mention its superior BER performance compared to MMSE scheme of (Natarajan et al; 2001). The performance improvement for the proposed subcarrier PIC is due to the twofold advantages in interference cancelation. Since the high data rate transmission uses all sub-carriers, the data can be decoded with greater reliability and interference due to these users can be estimated with greater accuracy. This interference when subtracted from the resultant received signal improves detection performance of the low data rate users. On the other hand, low data rate transmission uses alternate sub-carriers, so subcarriers of high data rate users experience less interference that leads to an improvement in BER performance of the latter. This cumulative effect on BER performance in multistage interference cancelation significantly improves overall BER performance of the proposed system unlike to that of the block PIC scheme in (Thippavajjula; 2004). In block PIC, in any stage

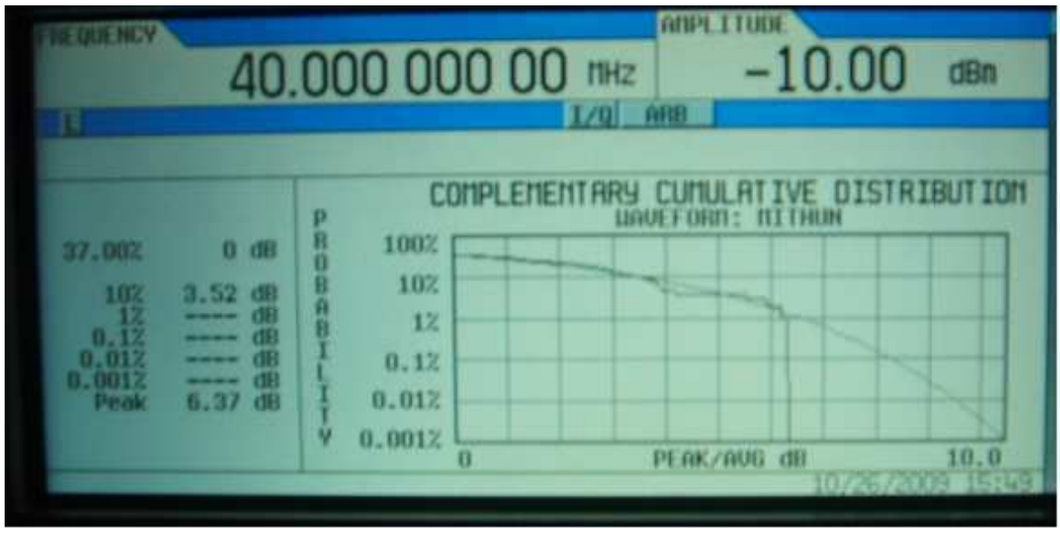

Fig. 7. CCDF of PAPR in QPSK for N=24 before code and phase optimization

Sl. no	N	K	SNR	PAPR	BER	ADR
1	25	54	14	18.6040	0.0770	1.000
2	23	48	14	16.0504	0.0691	1.0000
3	21	44	13	14.1088	0.0805	1.0000
4	20	35	10	13.1250	0.0691	1.0000
5	22	43	12	15.3944	0.0714	1.0000
6	18	33	11	13.1597	0.0670	1.0000
7	24	46	10	16.9413	0.0683	1.0000

Table 3. GA based optimization in

of interference cancelation, weak users data noway benefits BER performance of strong users data unlike the proposed subcarrier PIC scheme.
Fig. 18 shows graphical representation for BER performance with the number of users for subcarrier parallel interference cancelation (PIC) (Maity & Mukherjee; 2009), code and subcarrier PIC and trellis coded system for 'N'=16 and SNR=14 dB. It is found that trellis coded system provides significant improvement in BER performance even at less number of interference cancelation stage compared to the same for higher stage interference cancelation of subcarrier PIC and combined code & phase PIC.

5.4 Performance evaluation of optimized system

Table 2 and Table 3 show the performance of the optimization for the proposed system and CI/MC-CDMA system in (Natarajan et al; 2001), respectively. Simulation results clearly specify the importance of the optimization problem. The values of PAPR, BER and ADR for both the optimized systems are quite consistent for the particular combinations of K, N and SNR values i.e. large N values offer lower BER and increased data transmission rate, while large K values yield increased BER. The values of SNR have both way effect on BER performance in multiuser communication system. As a matter of fact, a set of N, K, SNR values are (at least) near optimal for the set of PAPR, BER and ADR values with respect to the status of the wireless channel condition. For example, if we see the results depicted in 4th row (Sl. no 3)

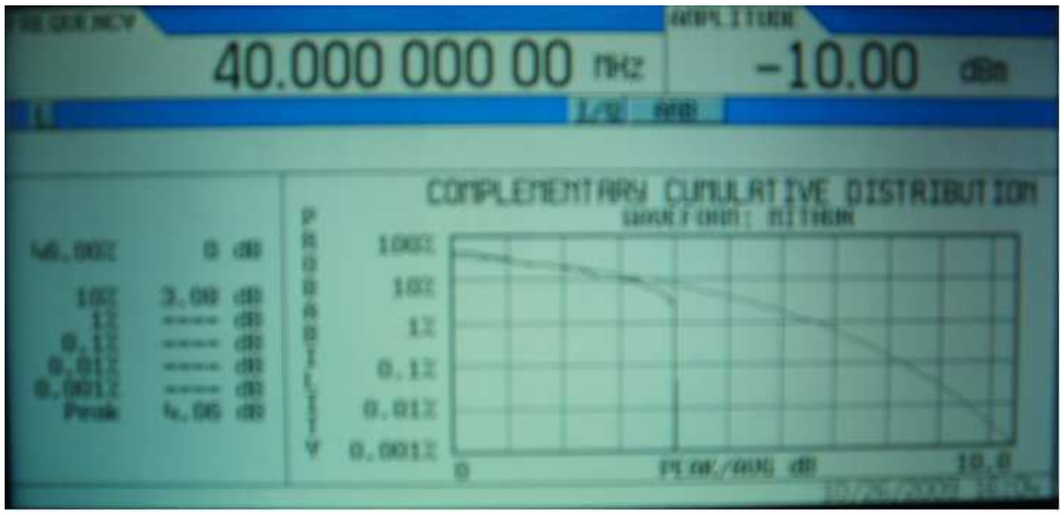

Fig. 8. CCDF of PAPR in QPSK for N=24 after code and phase optimization

of Table 2 and Table 3, for N=21, and for similar SNR values (14 dB for the proposed system and 13 dB for (Natarajan et al; 2001)), PAPR values of proposed system is lower compared to (Natarajan et al; 2001) due to improved PAPR reduction performance for the proposed system. At the same time a significant improvement in BER is achieved for our method due to novelty of the proposed subcarrier scheme, even at nearly 1.5 times increase in user capacity. Similar explanation is applicable for other set of results in Table 2 and Table 3.

6. Conclusion

This chapter discusses a new model of high capacity CI/MC-CDMA system with variable data rates along with simple, fast and efficient PAPR reduction at transmitter and subcarrier PIC scheme at receiver. PAPR reduction is achieved through phase shift of pseudo-orthogonal codes with respect to the orthogonal spreading codes assigned for low and high data rate transmission, respectively. The algorithm has been extended for M-ary PSK system. Significant reduction in PAPR is achieved with combined code and phase optimization in conjunction with trellis coding. Simulation results show that code optimization is more effective for PAPR reduction in BPSK, Q-PSK and 8-ary PSK while phase optimization is effective for the same in case of 16-ary PSK. In the receiver, a simple, fast and efficient subcarrier PIC scheme is proposed. BER performance of the proposed method not only shows improved result compared to the conventional PIC and block PIC system but also requires low computation complexity. The scope of usage of genetic algorithms for the estimation of channel parameters for the proposed MC-CDMA system is then explored. The results reported here show that with the increase of number of users, BER values corresponding to the estimated parameters closely follow to that of BER values obtained for actual parameters values. Simulation results also show that with the increase of number of generations both BER values decrease and channel capacity increases. Finally, GA based optimized system is designed to achieve acceptable values of PAPR, BER and ADR for optimal set of the number of users, the number of subcarriers and SNR values based on the status of the wireless channel.The prposed system may be used as a potential multiple access with broadband data transmission for both uplink and downlink satellite system in conjunction with mobile communication.

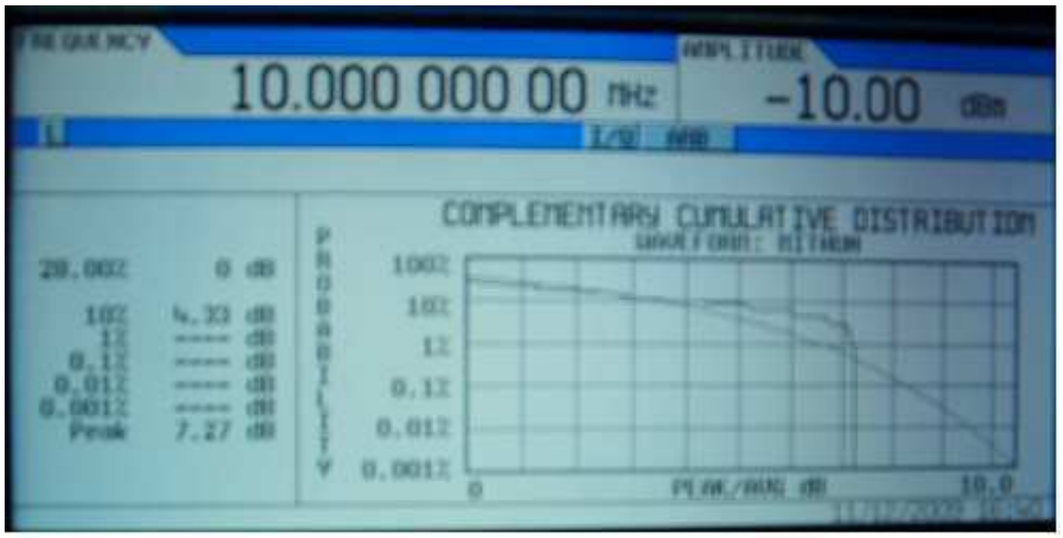

Fig. 9. CCDF of PAPR in 8-ary PSK for N=24 before code and phase optimization

Fig. 10. CCDF of PAPR in 8-ary PSK for N=24 after code and phase optimization

Acknowledgment

The author acknowledge financial support for the project on "Development of high power and spectral efficiency multiuser system for broadband wireless communication" funded by Ministry of Communication and Information Technology, Govt. of India vide administrative approval no. 13(2)/2008-CC & BT dated 31.03.2008.

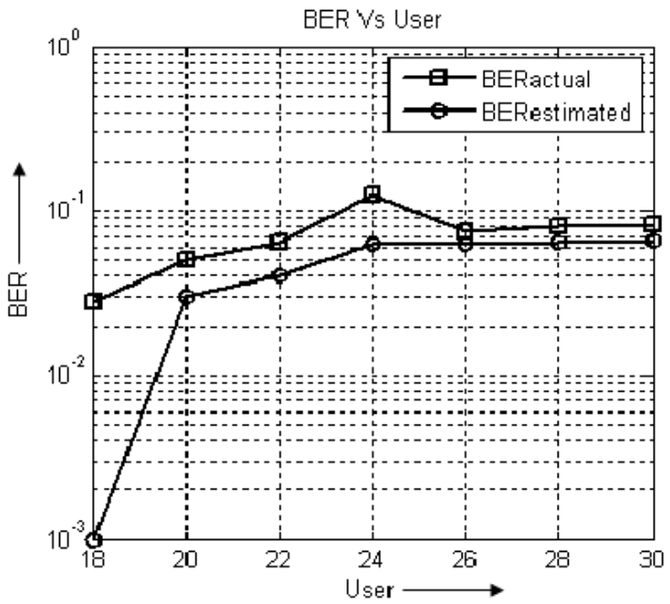

Fig. 11. BER comparison for estimated and actual channel parameters

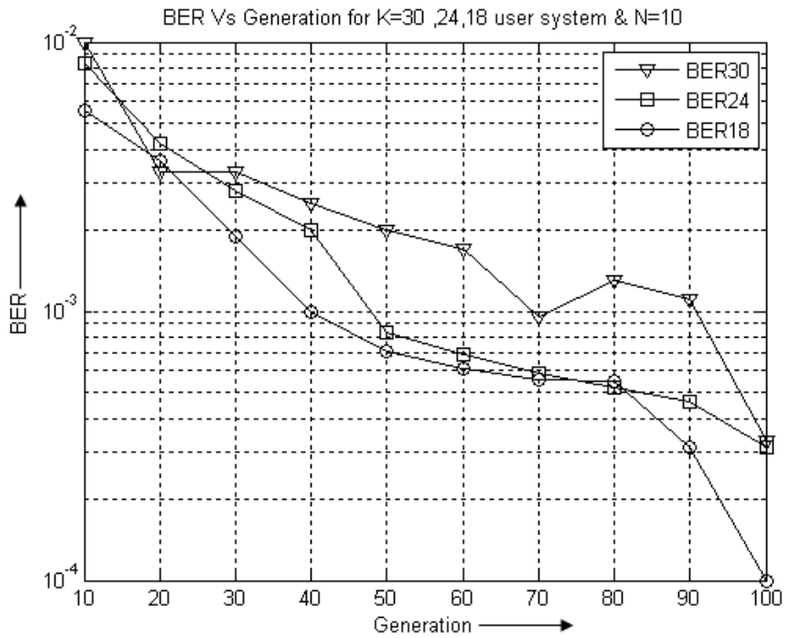

Fig. 12. BER performance with the number of generations

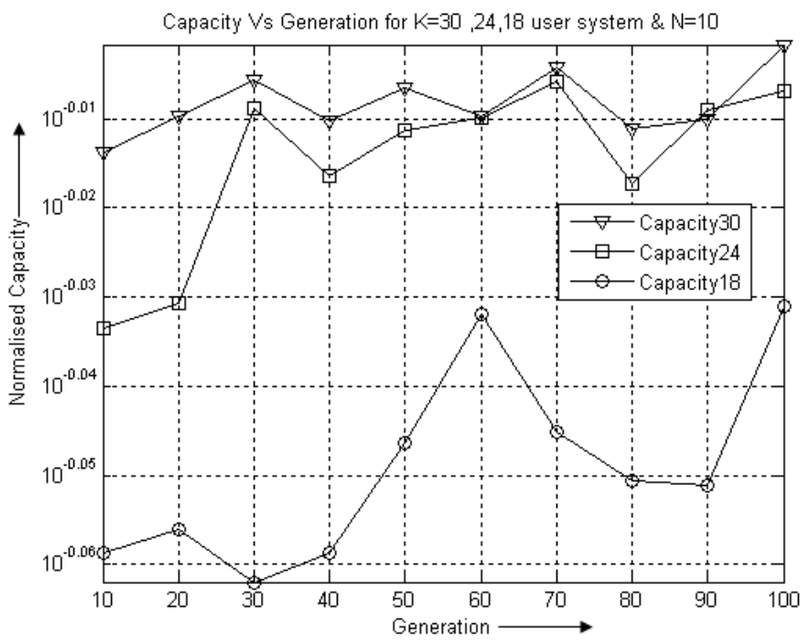

Fig. 13. Channel capacity with number of generations

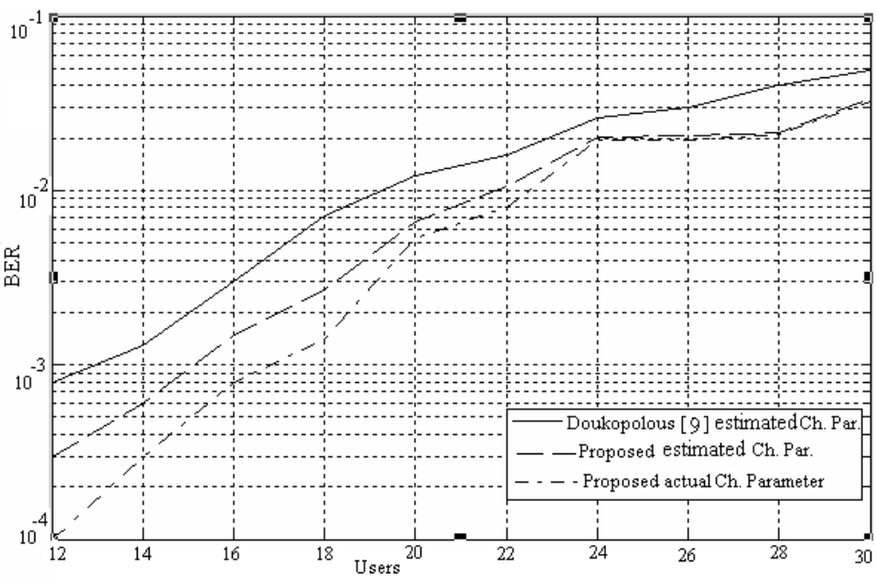

Fig. 14. Comparison of BER performance through channel estimation using N=10 and SNR=7dB

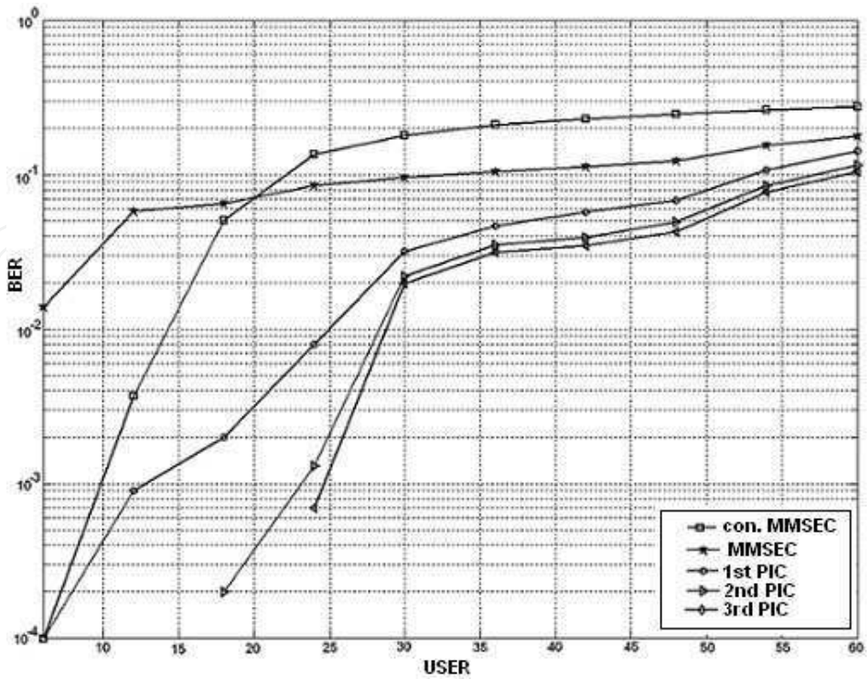

Fig. 15. Performance of subcarrier PIC scheme for 3N user system

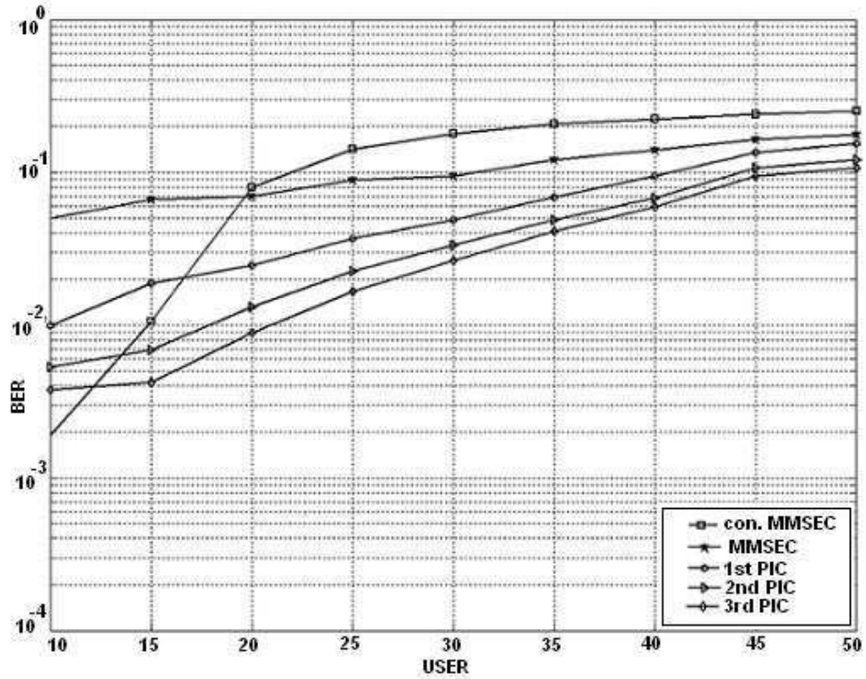

Fig. 16. Performance of subcarrier PIC scheme for 2.5N users system

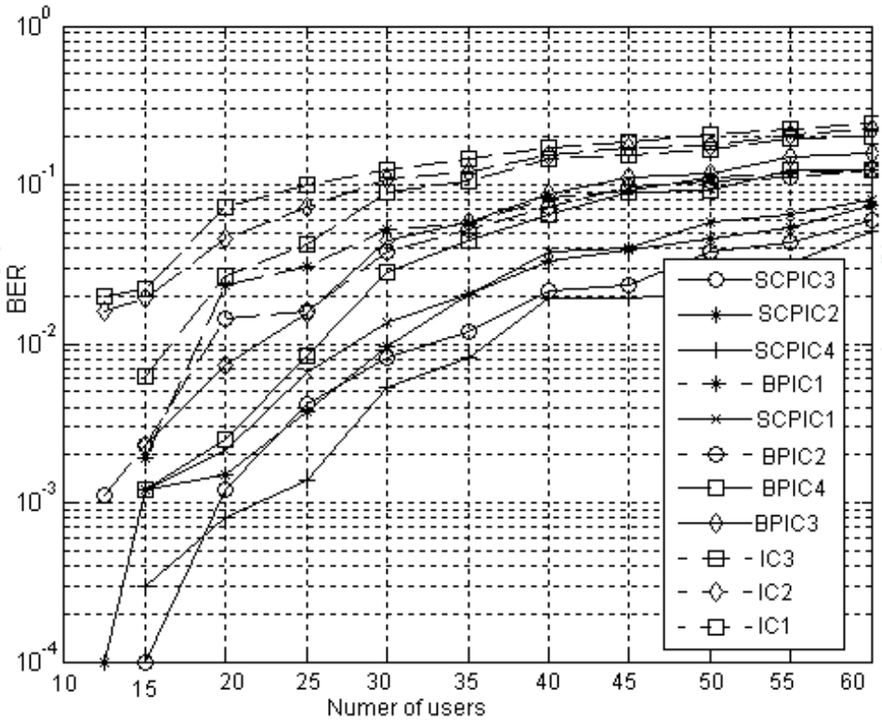

Fig. 17. Performance comparison of subcarrier PIC & block PIC schemes for 3N users system

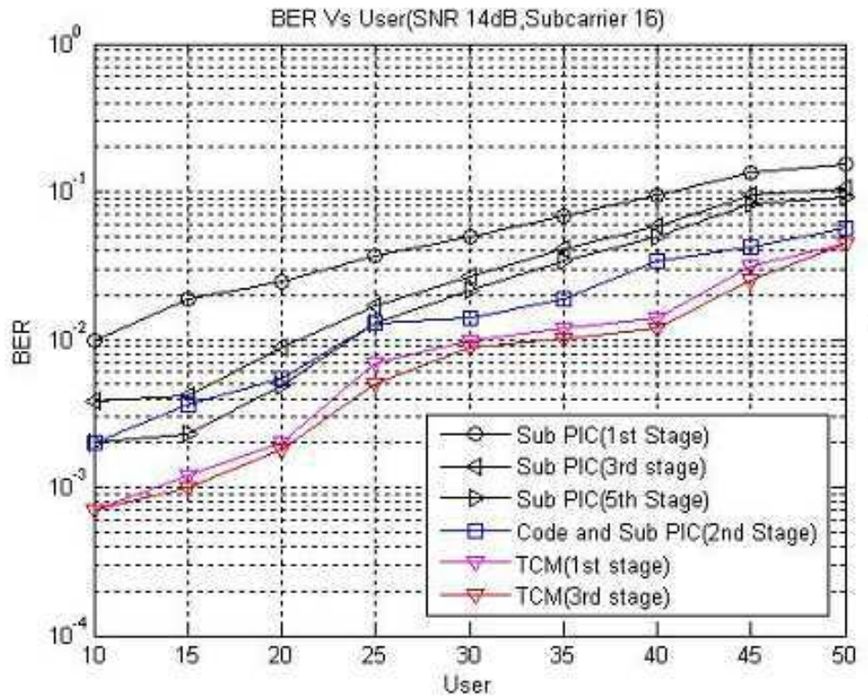

Fig. 18. BER performance for subcarrier PIC, Code and subcarrier PIC and trellis coded system for N=8 and K=24

7. References

Ochiai H. and Ima H.(2000). Performance of the deliberate clipping with adaptive symbol selection for strictly bandlimited OFDM systems. *IEEE Journal on Selected Areas in Communications*, Vol. 18, No. 11, (2000) (2270-2277)

Lim D. W., Heo S. J., No J. S., and Chung, H. A New PTS OFDM Scheme with Low Complexity for PAPR Reduction. *IEEE Tran. Broadcasting* Vol. 52, No. 1, (2006)(77-82).

Yoo, S., Yoon, S., Kim S. Y. and Song, I. A novel PAPR reduction scheme for OFDM systems: Selective Mapping of Partial Tones (SMOPT). *IEEE Trans. on Consumer Electronics*, Vol. 52, No. 1, (2006) (40-43)

Ochia, H. A novel trellis-shaping design with both peak and average power reduction for OFDM systems. *IEEE Trns. on Communication*, Vol. 52, No. 11, (2004)(1916-1926).

Kang, K., Kim, S., Ahn, D. and Lee, H.J. Efficient PAPR reduction scheme for satellite MC-CDMA systems, *IEE Proc. on Communication*, Vol. 152, No. 5, (2005)(697-703).

Vedu, S. Minimum probability of error for asynchronous gaussian multiple access channels. *IEEE Transactions on Inform. Theory*, Vol. 32, (1986)(85-96)

Lupas, R. and Verdu, S. Linear multiuser detectors for synchronous code division multiple access channels. *IEEE Transactions on Inform. Theory*, Vol. 35,(1989)(123-136)

Divsalar, D., Simon, M. K. and Raphaeli, D. Improved Parallel Interference Cancelation for CDMA. *IEEE Trans. Communication*, Vol. 46, No. 2 (Feb 1998)(258-268)

Kim, S. and Lee, J. H. Performance of iterative multiuser detection with a partial PIC detector and serial concatenated codes, *IEEE VTS 54th Vehicular Technology Conference*, Vol. 1, pp.487-491, 2001.

Xiao, L. and Liang, Q. The study of parallel interference weighted canceler multiuser detection, *IEEE VTS 50th Vehicular Technology Conference*, Vol. 5,pp.3009-3013, 1999.

Thippavajjula, V. and Natarajan, B. Parallel interference cancelation techniques for synchronous carrier interferometry/MC-CDMA uplink, *IEEE Vehicular Technology conference*,pp.399-403, 2004.

Maity, S. P., Hati, S. and Maity, S. Diversity Assisted Block PIC for Synchronous CI/MC-CDMA Uplink Systems Using Genetic Algorithm, *Proceedings of the third IEEE International Conf. on Industrial and Information System*, Indian Institute of Technology, Kharagpur, India, (December 2008).

Sgraja, C. and Linder, J. Estimation of Rapid Time- Variant Channels for OFDM using Wiener Filtering, Proc. IEEE Int. Conf.on Comm., Vol. 4, pp. 2390-95, 2003.

Chow, J. S., Tu, J. C. and Cioffi, J. M. A discrete multitone transceiver system for HDSL application. *IEEE J. Select.Areas Communication*, Vol. 9,(Aug. 1991)(895Ű-908).

Ziegler, R. A. and Cioffi, J. M. Estimation of time-varying digital radio channel. *IEEE Trans. Veh. Tech.*, Vol. 41, (1992)(134Ű-151).

Wang, X. and Ray Liu, K. J. Adaptive channel estimation using cyclic prefix in multicarrier modulation system. *IEEE Commun. Lett.*, Vol. 3, No. 10, (1999)(291-293).

Choi, Y. S., Voltz, P. J. and Cassara, F. A. On channel estimation and detection for multicarrier signals in fast and selective Rayleigh fading channels. *IEEE Trans. on Communication*, Vol. 49, No. 8,(2001)(1375-1387).

S. Coleri, M. Ergen and A. Puri, A study of channel estimation in OFDM systems, IEEE Globecom, 2002.

P. Schramm and R. Mullar, Pilot symbol assisted on Rayleigh fading channels with diversity: Performance analysis and parameter optimization. *IEEE Trans. on Communication*, Vol. 46, No. 12, (1998)(1560-1563).

Doukopoulos X. G. and Moustakides, G. V. Blind adaptive channel estimation in OFDM systems, *Proc. Of IEEE ICC*, Vol. 4, (2004)(20-24).

Gupta, P. and Mehra, D. K. Kalman filter based equalization for ICI suppression in High mobility OFDM systems, *Proc. of 13th National Conf. on Commun.*, (NCC-07), IIT Kanpur, pp.21-25, 2007.

Ramesh, C., Jawakar P. K., and Vaidehi, V. Pilot based adaptive channel estimation for OFDM system using GS FAP algorithm, *Proc. of 12th National Conf. on Commun. (NCC-2006)*, IIT Delhi, pp. 94-98, 2006.

Gao, X., Jiang, B.,You, X., Pan, Z., Xue, Y. and Schulz, E. Efficient Channel Estimation for MIMO Single-Carrier Block Transmission With Dual Cyclic Timeslot Structure. *IEEE Trans. on Communications*, Vol. 55, no. 11, (November 2007), (2210-2223).

Lok, T. M. and Wong, T. F. Transmitter and Receiver Optimization in Multicarrier CDMA Systems. *IEEE Transaction on Communication*, (2000)(1197-1207).

Wu, Q. Performance of optimum transmitter power control in CDMA cellular mobile systems. *IEEE Transaction on Vehicular Tech.*, Vol. 48, (1999).

Reynolds, D. and Wang, X. Adaptive transmitter optimization for blind and group-blind multiuser detection. *IEEE Trans. on Signal Proc.*, Vol. 51, (2003)(825-38).

Kim, D. Rate-regulated power control for supporting flexible transmission in future CDMA mobile networks. *IEEE Journal on Selected Areas Commmunications*, Vol. 17, (1999)(968-977).

Buzzi, S. and Poor, H. V. Joint Transmitter and Receiver Optimization for Energy-Efficient CDMA Communications. *IEEE Journal Selected Areas Communication -Special issue on multiuser detection for adv. commun. and networks*, Vol. 26,(Apr. 2008)(pp. 459-472).

Seo, K. and Yang, L. Joint transceiver optimization in MC-CDMA systems exploiting multipath and spectral density, *IEEE GLOBECOM Proceedings*, pp. 1-5, 2006.

Yee, N., Linnartz, J. P. and Fettweis, G. BER of multicarrier CDMA in indoor wireless networks. *IEEE Trans. on Commun.*, Vol. 1, (1993)(2817-2821).

Natarajan, B., Nassar, C.R., Shattil, S., Michelini, M. and Wu, Z. High performance mc-cdma via carrier interferometry codes. *IEEE Transactions on Vehicular Technology*, Vol. 50, (2001)(1344-1353).

Maity, S. P., Hati, S., Maity, S. and Mandal, M. K. Transmitter Optimization in Diversity Assisted Synchronous CI/MC-CDMA Uplink Systems Using Genetic Algorithm, *24th IEEE Queen's Biennial Symposium on Communications (QBSC-2008)*, Canada, pp. 62-67, 2008.

Proakis, J.G. *Digital communications*, 3rd Ed,McGraw-Hill, 1995.

Cal, X. and Akansu, A. N. Multicarrier CDMA systems with transmit diversity. *IEEE Transactions on Vehicular Technology*, Vol. 2, (2000)(658-661)

Ahamad, A. and Ali Assaad, M. Margin adaptive resources allocation in downlink OFDMA system with outdated channel state information, *PIMRC 2009*, Japan.

Doukopoulos, X. G. and Moustakides, G. V. Blind adaptive channel estimation in OFDM systems, *Proc. Of IEEE ICC*, Vol. 4, pp. 20-24, 2004.

Maity S. P. and Mukherjee M., Subcarrier PIC scheme for high capacity CI/MC-CDMA System with Variable Data Rates, IEEE Mobeile WiMAX'09, July 9-10, Napa Valley, California, pp. 135-140, 2009.

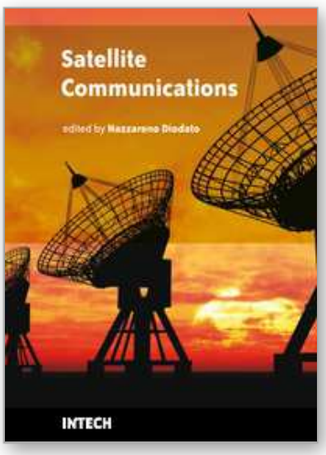

Satellite Communications

Edited by Nazzareno Diodato

ISBN 978-953-307-135-0

Hard cover, 530 pages

Publisher Sciyo

Published online 18, August, 2010

Published in print edition August, 2010

This study is motivated by the need to give the reader a broad view of the developments, key concepts, and technologies related to information society evolution, with a focus on the wireless communications and geoinformation technologies and their role in the environment. Giving perspective, it aims at assisting people active in the industry, the public sector, and Earth science fields as well, by providing a base for their continued work and thinking.

How to reference

In order to correctly reference this scholarly work, feel free to copy and paste the following:

Santi Maity (2010). Power and Spectral Efficient Multiuser Broadband Wireless Communication System, Satellite Communications, Nazzareno Diodato (Ed.), ISBN: 978-953-307-135-0, InTech, Available from: http://www.intechopen.com/books/satellite-communications/power-and-spectral-efficient-multiuser-broadband-wireless-communication-system

INTECH
open science | open minds

InTech Europe
University Campus STeP Ri
Slavka Krautzeka 83/A
51000 Rijeka, Croatia
Phone: +385 (51) 770 447
Fax: +385 (51) 686 166
www.intechopen.com

InTech China
Unit 405, Office Block, Hotel Equatorial Shanghai
No.65, Yan An Road (West), Shanghai, 200040, China
中国上海市延安西路65号上海国际贵都大饭店办公楼405单元
Phone: +86-21-62489820
Fax: +86-21-62489821

IntechOpen